Biomedical Engineering Letters
https://doi.org/10.1007/s13534-024-00422-y

ORIGINAL ARTICLE

Assessment of conductive textile-based electrocardiogram measurement for the development of a lonely death prevention system

Lina Agyekumwaa Asante[1] · Sung Bin Park[2] · Seungkwan Cho[3] · Jun won Choi[1] · Han Sung Kim[4]

Received: 18 June 2024 / Revised: 18 June 2024 / Accepted: 8 August 2024

Abstract
The rise in individuals living alone in ageing societies raises concerns about social isolation and associated health risks, notably lonely deaths among the elderly. Traditional electrocardiogram (ECG) monitoring systems, reliant on intrusive and potentially irritating electrodes, pose practical challenges. This study examines the efficacy of conductive textile electrodes (CTEs) vis-á-vis conventional electrodes (CEs) in ECG monitoring, along with the effect of electrode positioning. Twenty subjects without cardiovascular conditions, were monitored using a commercial ECG device (HiCardi+) with both CEs and CTEs. The CTEs were tested in two experiments: at the nape and left hand (position 1), and at the nape and legs (position 2). Each experiment placed one HiCardi + SmartPatch with CE at its standard position, while the other used CTEs. ECG signals were processed using the Pan-Tompkins algorithm, and heart rate variability (HRV) metrics were analysed. Significant improvements in signal-to-noise ratio (SNR) were observed after filtering. There were no significant differences ($p > 0.05$) in time-domain HRV metrics between CEs and CTEs, though CTEs showed superior R peak characteristics and reduced noise sensitivity. Additionally, no significant position effect ($p > 0.05$) was noted within the CTE group. Nonlinear analysis further confirmed the efficacy of the CTEs. Our findings suggest that CTEs offer a comfortable, non-intrusive alternative to conventional ECG electrodes, enhancing ECG monitoring and contributing to the development of a "lonely death prevention system".

Keywords Lonely deaths · Conductive textile electrodes (CTEs) · Electrocardiogram (ECG) · Heart rate variability (HRV)

1 Introduction

As societies witness an increasing trend of people living alone, concerns arise regarding potential social isolation and health hazards, especially the risk of lonely deaths. This demographic shift is becoming more pronounced with ageing populations, emphasising the need to address unique healthcare challenges faced by those living alone. Lonely deaths, also known as solitary deaths, occur when an individual dies in isolation and their remains are not discovered for an extended duration [1]. This phenomenon has sparked discourse in Western societies, on whether it should be regarded as an unfavourable end or a demonstration of self-determination [2–4].

In Asia, particularly in Japan (referred to as "孤独死" (kodokushi)) and South Korea ("고독사" (godoksa)), these occurrences are common. In recent times, the issue of lonely deaths has surged as a notable social concern in South Korea [5–7]. Individuals in this group, especially the elderly, often exhibit low awareness of healthcare needs or limited access to medical services. Among the health-related factors this demographic grapples with, cardiovascular health is critical, worsened by the prevalence of sleep-related cardiac issues. Despite advancements in healthcare technology, detecting and addressing these matters remain challenging.

✉ Han Sung Kim
hanskim@yonsei.ac.kr

1 Department of Biomedical Engineering, Yonsei University, Wonju-si, Gangwon-do 26493, Republic of Korea

2 Department of Precision Medicine, Yonsei University Wonju College of Medicine, 20, Ilsan-ro, Wonju-si, Gangwon-do, Republic of Korea

3 GFYHealth Inc., 20, Pangyo-ro 289, Bundang-gu, Seongnam-si, Gyeonggi-do 13488, Republic of Korea

4 Department of Biomedical Engineering, Yonsei University College of Software and Digital Healthcare Convergence, Wonju-si, Gangwon-do 26493, Republic of Korea

Current approaches to cardiovascular monitoring and management often rely on conventional electrocardiogram (ECG) monitoring systems. However, such methods may pose practical difficulties due to their intrusive nature and requirement for adhesive electrodes. Electrodes, pivotal components of the ECG system [8], translate physiological signals into meaningful data. In clinical settings, disposable silver/silver chloride (Ag/AgCl) wet electrodes are commonly used due to their high signal quality. Nonetheless, these electrodes are prone to drying out over time, increasing the risk of data loss [9], diminished signal quality and could also induce dermatitis [10]. These limitations necessitate frequent replacements and specific skin preparation procedures [11, 12].

Given the intertwined relationship between living alone, social isolation, and cardiovascular health, there is a pressing need for innovative monitoring and management solutions. Wearable health monitoring technologies have driven the demand for more comfortable and user-friendly electrodes, such as ECG patch monitors. Yet, these devices can sometimes be difficult to apply correctly, potentially compromising measurement accuracy.

Conductive textile electrodes (CTEs) have recently garnered attention as prospective solutions for ECG monitoring. Composed of conductive fibres or coatings integrated into textile substrates, CTEs have been used for wearable biopotential signal monitoring owing to their breathability, flexibility and comfortability [13, 14]. They exhibit low impedance and stable electrical properties, ensuring reliable signal acquisition over extended periods.

While literature have illustrated the efficacy of CTEs in physiological signal acquisition [15–17], a notable paucity exists in understanding their signal disparities compared to conventional electrodes (CEs). In this study, we assess the efficacy of CTEs for ECG measurement compared to CEs by analysing their ECG morphologies and time-series heart rate variability (HRV) data. We further identify the most suitable electrode position for CTEs. This work aims to contribute to advancements in ECG electrode technology, particularly in developing an integrated system to prevent lonely deaths among the elderly population.

2 Materials and methods

2.1 Subjects

Twenty subjects (6 females and 14 males), devoid of pre-existing cardiovascular pathologies or factors possibly influencing ECG measurements, were enlisted for the study. Their demographic characteristics were, mean age of 28.10 ± 6.46 years, average weight of 73.92 ± 16.45 kg and mean height of 170.18 ± 8.95 cm. Prior to commencing, each subject provided their informed consent in compliance with ethical procedures. This process provided detailed information regarding the experimental procedures to ensure comprehension and voluntary participation.

2.2 ECG recording device

ECG signals were acquired using a commercial device—HiCardi+ (MEZOO Co. Ltd., Gangwon-do, Korea). The HiCardi+ is a two-point leadless, single-channel ECG monitoring device accredited by the Ministry of Food and Drug Safety of Korea. With a weight of 18 g and dimensions, 6 cm $\times$ 4 cm $\times$ 1 cm, its signal acquisition occurs at a sampling frequency of 250 Hz and a resolution of 16 bits. The HiCardi+ ECG monitoring patch is capable of detecting arrhythmias, temperature, activity, respiration, and body posture of neonates, infants, paediatrics and adults. Utilising Bluetooth low energy, data captured by the device are seamlessly transmitted to a mobile gateway, integrated within the SmartView smartphone application. Subsequently, all data are forwarded by the mobile gateway to a cloud-based monitoring server, LiveStudio, for analysis.

2.3 Electrode placement

Each subject assumed a supine posture with their arms slightly extended from their bodies at about an angle of 10°. Two types of electrodes were subjected to comparison: Ag/AgCl ECG electrode (MEZOO Co. Ltd., Gangwon-do, Korea) referred herein as CE and CTE (Cellogin Co., Ltd., Wonju, Korea). The CTE has a thickness of 0.025 cm and is made from a combination of graphite and graphene composite powder—thus, it is known to have excellent electrical and thermal conductivity. Skin-preparations were carried out to ensure the adherence of the CEs. Two experiments were conducted, each utilising two HiCardi+ devices. Each experiment involved the placement of one HiCardi+ SmartPatch with CE at its standard position, while the other was affixed with CTEs at the nape and left hand (position 1), and subsequently at the nape and legs (position 2). The dimensions of the CTEs were customised as follows: pillow (103 cm $\times$ 50 cm), left-hand (75 cm $\times$ 41 cm), and legs (149 cm $\times$ 41 cm). After positioning the CTEs, the subjects laid on them, and adjustments were made individually to ensure proper contact.

2.4 ECG experimental design

Standard protocols for short-term HRV assessment recommend a 5-min recording period, preceded by a 5-min stabilisation phase in the supine position [18]. This phase is critical for stabilising heart rate, reducing the impact of prior physical activity, and ensuring accurate HRV measurements by minimising potential confounding variables. Following the electrode attachments, subjects remained still for approximately 5 min before ECG data collection commenced. Throughout the 20-min recording session, subjects closed their eyes to simulate a sleep-like state. This approach was to minimise visual distractions and mental activity. In addition to being informed beforehand, the brief duration and controlled environment were designed to further minimise the likelihood of actual sleep. The experiment concluded after data collection, with an additional 5-min break provided if any signs of dizziness indicative of orthostatic hypotension were observed.

2.5 ECG measurement

ECG data was collected concurrently using CEs and CTEs in both experiments as illustrated in Fig. 1. To extend the connection from the HiCardi+ device to the CTEs, alligator clips with wires were stuck into the device's attachment points. Secure connections and insulated wires were implemented to prevent noise, while careful positioning reduced movement. Preliminary testing confirmed signal reliability and consistency. The ECG signals were recorded in a quiet environment with regulated lighting and temperature to reduce the impact of outside factors.

2.6 Signal processing and analysis

With the assistance of MEZOO Co. Ltd., the raw ECG data from the HiCardi + devices were retrieved. The files contained the timestamps and their corresponding voltage values representing the ECG signals. HRV data retrieval and denoising of ECG signals were handled in the pre-processing phase. The Pan-Tompkins algorithm [19] was applied to identify the QRS complexes using MATLAB (version R2023b, MathWorks, Natick, MA, USA). This involved applying a sequence of filters to reduce noise and highlight the quick changes of voltage in the QRS phase.

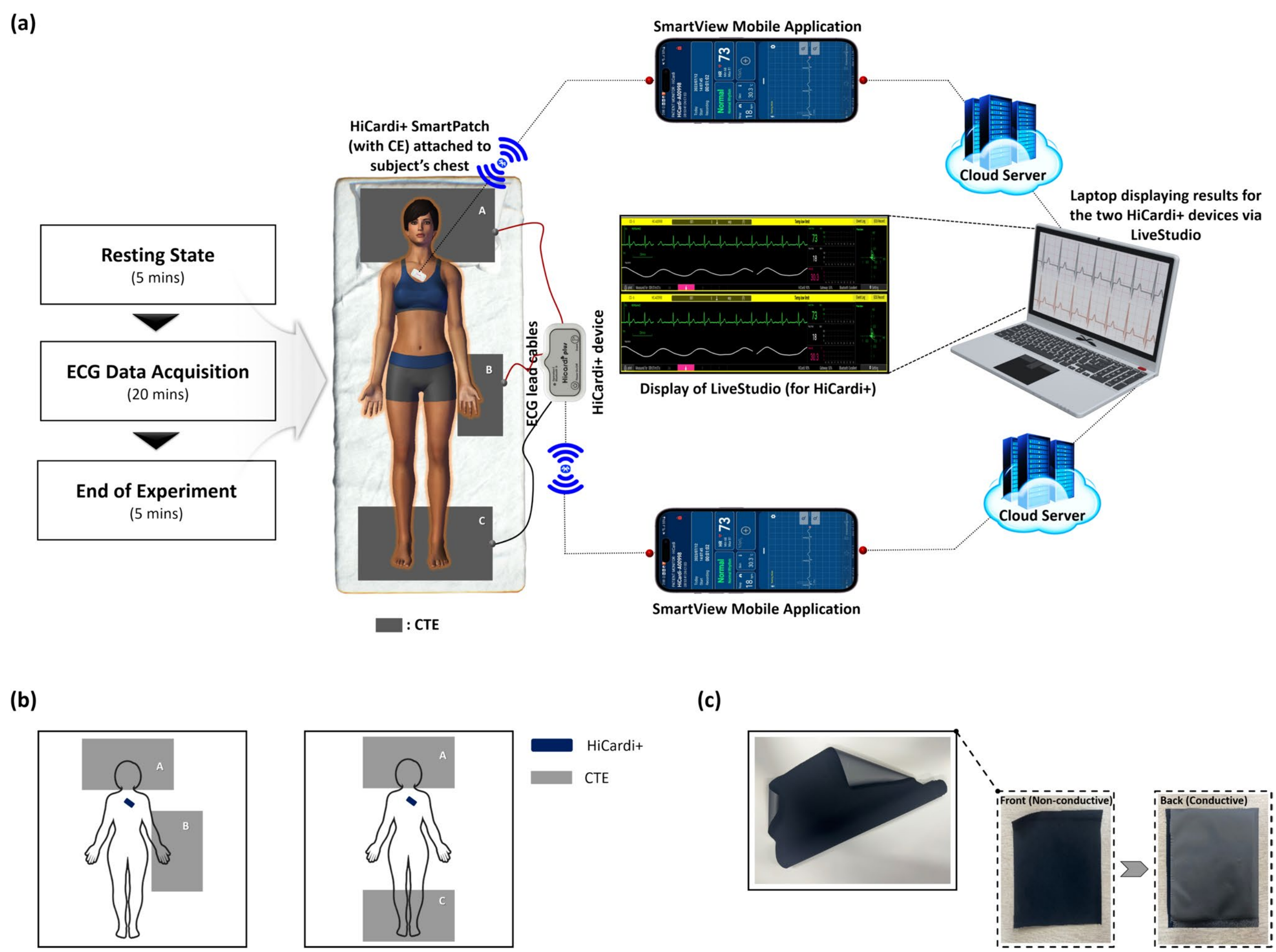

Fig. 1 Schematic representation of the **a** ECG measurement setup and data acquisition using CEs and CTEs in the two positions. **b** Electrode positions **c** Digital photo of the CTE

The first stage of this sequence was filtering. In our analysis, a second-order Butterworth infinite impulse response filter with a passband between 5 and 15 Hz was applied to improve the signal quality using:

$$H(s) = \frac{1}{1 + \left(\frac{s}{\omega_c}\right)^{2n}} \quad (1)$$

where, $H(s)$ is the transfer function of the filter, s is the complex frequency variable, ω_c is the cut-off frequency and n is the order of the filter.

The peaks in the ECG waveform were then located by computing the derivative of the filtered signal using Eq. (2). A polynomial regression within a moving window of data points was employed to approximate the derivative of the original signal using a Savitzky-Golay filter [20].

$$\frac{dy}{dt}[n] = \sum_{i=0}^{N-1} C[i] \cdot y[n-i] \quad (2)$$

where, $\frac{dy}{dt}[n]$ is the derivative of the signal at time index n

$C[i]$ is the $i-$th coefficients of the polynomial regression obtained through least squares fitting.

$y[n-i]$ is the value of the signal at time index $n-i$

The square of the derivative signal was then computed using Eq. (3) to amplify the amplitude of peaks in the ECG waveform.

$$y(t) = \left(\frac{dy}{dt}\right)^2 \quad (3)$$

The squared derivative signal was then subjected to a moving average window to smooth out variations and identify significant peaks. In our analysis, we used a window length corresponding to 5% of the sampling rate (250 Hz). The moving average of signal y(t) over a window of size N was calculated as:

$$MA(t) = \frac{1}{N}\sum_{i=o}^{N-1} y(n-i) \quad (4)$$

where, $MA(t)$ is the moving average at time t, and $y(n-i)$ are the signal values within the window centered at time, t.

2.7 HRV feature extraction

To calculate the HRV parameters, RR intervals were first determined by measuring the geometric angle between two successive samples of the ECG signal. RR interval time series was then obtained using the identified R peaks. Quality control procedures were implemented to identify and exclude any data segments affected by artefacts or technical issues, ensuring that only reliable data were used in the analyses. Figure 2 depicts the framework for feature extractions.

2.7.1 Time-domain indices of HRV

HRV is predominantly evaluated in the time-domain using statistical metrics derived from inter-beat intervals [21] or RR intervals. The analysis was performed using the Python programming language, specifically *BioSPPy* and *SciPy* packages, and the Hamilton-Tompkins algorithm [22]. Time-domain indices used in this study are discussed below:

The average RR interval (AvgRR) represents the average time between successive heartbeats (R waves in an ECG) and is calculated by dividing the mean value of the sum of the RR intervals by the total number of RR intervals.

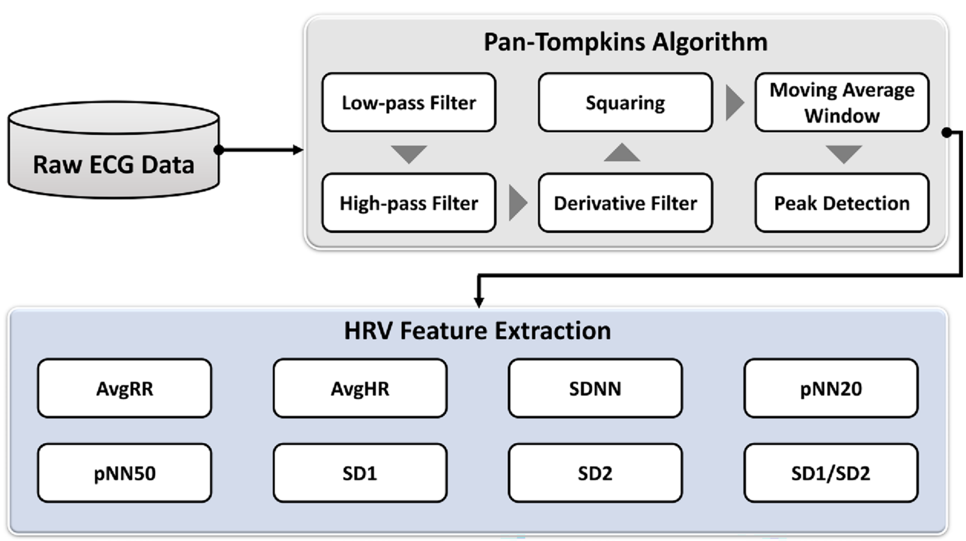

Fig. 2 Schematic diagram of the signal processing using the Pan-Tompkins algorithm and HRV feature extraction

$$AvgRR(ms) = \frac{1}{N}\sum_{i=1}^{N} RRi \tag{5}$$

where, N is the total number of elements of RRi during the time period.

The average heart rate (AvgHR), denoted as the mean value of heartbeats per minute within a specified time frame, is calculated by converting the reciprocal of the mean RR interval into beats per minute (bpm).

$$AvgHR(bpm) = \sum_{i=1}^{N}\left(\frac{60000}{RR_j}\right) \times 60 \tag{6}$$

Here, N represents the count of RR intervals and RR_j signifies the j-th RR interval.

The standard deviation of average normal-to-normal (NN) intervals (SDNN), is calculated as the square root of the mean of the squared differences between consecutive NN intervals.

$$SDNN(ms) = \sqrt{\frac{1}{N-1}\sum_{j=1}^{N}\left(RRi_j - \overline{RRi}\right)^2} \tag{7}$$

where, N is the count of RRi values, RRi_j is the j-th RRi value, and $\overline{RRi}$ is the average value of the RRi series.

pNN20, the percentage of successive NN intervals exceeding 20 ms is the proportion of NN intervals that differ by more than 20 ms ($nRRi_{20}$) to the total number of RRi (nRRi).

$$pNN20(\%) = \frac{nRRi_{20}}{nRRi} \times 100\% \tag{8}$$

The pNN50 akin to pNN20, quantifies the percentage of successive intervals exceeding 50 ms ($nRRi_{50}$) to the total number of RRi (nRRi).

$$pNN50(\%) = \frac{nRRi_{50}}{nRRi} \times 100\% \tag{9}$$

2.7.2 Quantitative beat-to-beat analysis of HRV

The correlation between successive RR intervals (RRn) is shown graphically in two dimensions by the Poincaré plot. On the x-axis, each interval is plotted against the succeeding ($RRn+1$) on the y-axis. It has been demonstrated that this plot is useful in offering qualitative insights into the complexity level of RR intervals in heart failure patients [23]. The Poincaré plot offers a quantitative assessment of HRV [24] defined by SD1, SD2 and SD1/SD2.

$$SD1 = \sqrt{Var(x_1)} \tag{10}$$

$$SD2 = \sqrt{Var(x_2)} \tag{11}$$

where, $x_1 = \frac{(RR_{i+} - RR_{i-})}{\sqrt{2}}$, $x_2 = \frac{(RR_{i+} + RR_{i-})}{\sqrt{2}}$

RR_{i+} is defined as (RR_1, R_2, …, RR_{N-1}) and RR_{i-} as (RR_2, RR_3, …, RR_N).

The parasympathetic modulation marker, SD1, denotes the instantaneous beat-to-beat variability [25]. Conversely, the variability in long-term continuous RR intervals is reflected by SD2, which serves as a marker for both sympathetic and parasympathetic regulation [26, 27]. Increased sympathetic modulation during progressive physical exercise is indicated by the SD1/SD2 ratio [21].

2.8 Statistical analysis

All continuous variables and demographic information were analysed using central tendency measures and frequency lists. A paired sample t-test was conducted to compare results from CEs and CTEs in both experiments. The position effect within the CTEs group was also analysed. For each time-domain index, normality of values in CTEs positions 1 and 2 was assessed using the Shapiro–Wilk test. If $p > 0.05$, normal distribution was assumed, and a one-sample t-test with a hypothetical mean of zero was selected to evaluate deviations from this baseline. This helped determine significant difference in time-domain indices relative to the reference, supporting the study's objective of assessing relative changes. For non-normal distributions, the Wilcoxon signed-rank test was applied. Statistical analyses were performed using IBM SPSS v.26.0 (IBM Corporation, Armonk, New York, USA), with significance set at $p < 0.05$ (two-sided). ECG signals and bar graphs were plotted using MATLAB and Prism 8 for Windows (GraphPad Software, Inc., La Jolla, CA, USA) respectively.

3 Results

3.1 ECG morphologies using CEs and CTEs

The first step in extracting relevant data from the ECG signals involved implementing noise reduction techniques to minimise extraneous interference. Hence, we focused on improving the signal-to-noise ratio (SNR) to enhance the fidelity of the acquired ECG waveform. Previous studies [28, 29] have shown that noise present in ECG recordings can markedly impact the precision of extracted HRV features. In light of this, the measured ECG signals underwent systematic signal processing methods using the Pan-Tompkins algorithm to elucidate the characteristic peaks

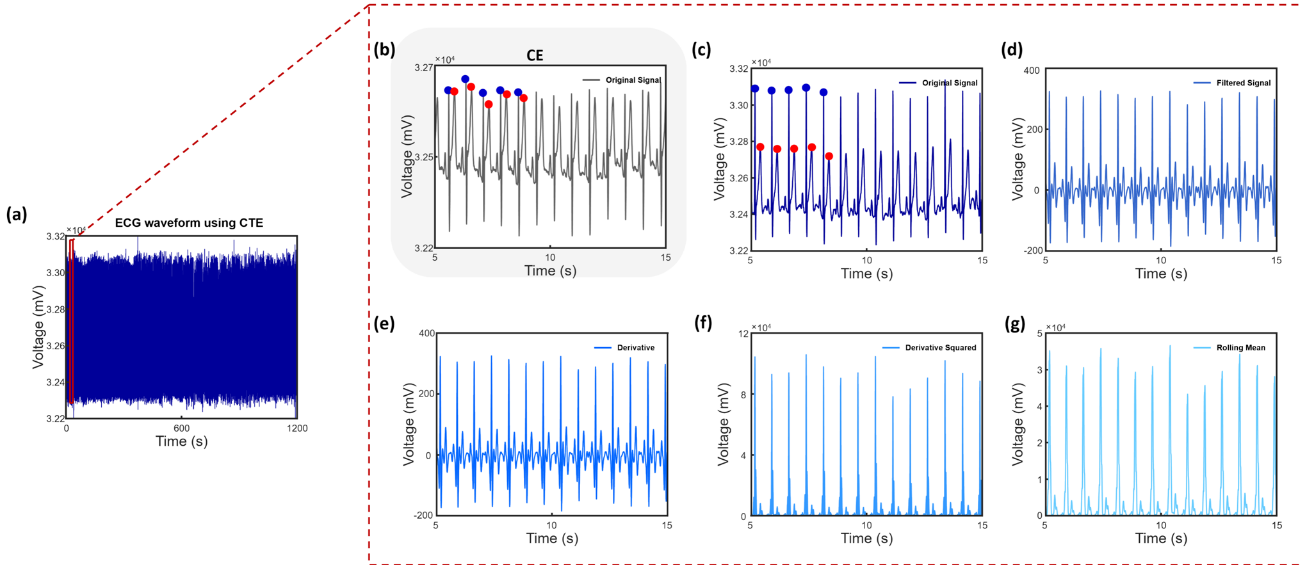

Fig. 3 Results of the signal processing of ECG waveforms obtained using CTEs in position 1. **a** Overall recorded ECG signal for a duration of 1200 s. Signals from the raw data for **b** CE and **c** CTEs. Signals from the processed data using the Pan-Tompkins algorithm for **d** filtered **e** derivative **f** derivative squared and **g** rolling mean. The R peaks are indicated by blue dots whilst the T peaks, red

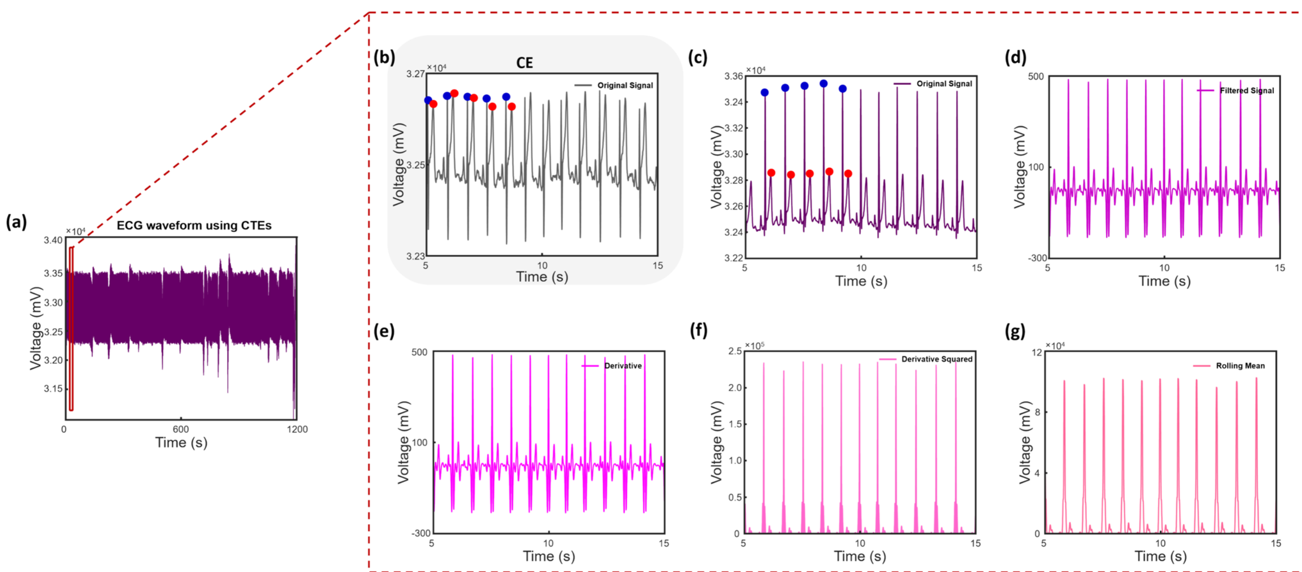

Fig. 4 Results of the signal processing of ECG waveforms obtained using CTEs in position 2. **a** Overall recorded ECG signal for a duration of 1200 s. Signals from the raw data for **b** CE and **c** CTEs. Signals from the processed data using the Pan-Tompkins algorithm for **d** filtered **e** derivative **f** derivative squared and **g** rolling mean. The R peaks are indicated by blue dots whilst the T peaks, red

of the waveforms. Notably, no skin preparations were conducted before applying our proposed CTEs. Figures 3 and 4 show the resulting ECG morphologies using CTEs after signal processing. Moreover, the raw signals obtained using CEs are also shown.

3.2 Sensor effect of CEs and CTEs

The results in the present study were analysed using time-domain indices of HRV. The results (mean ± standard deviation) for each metric are displayed in Table 1, along with the

Table 1 Time-domain indices of HRV recorded using CEs and CTEs in positions 1 and 2

	Position 1		*p* value	Position 2		*p* value
	CEs	CTEs		CEs	CTEs	
AvgRR (ms)	857.88 ± 144.74	830.25 ± 353.32	0.72	814.73 ± 302.05	911.52 ± 695.72	0.51
AvgHR (bpm)	71.94 ± 12.92	73.51 ± 30.12	0.82	60.66 ± 22.35	56.02 ± 27.02	0.49
SDNN (ms)	116.58 ± 61.11	111.85 ± 156.90	0.89	88.99 ± 38.84	68.46 ± 77.61	0.26
pNN20 (%)	77.50 ± 13.38	75.95 ± 23.23	0.73	71.35 ± 21.75	74.65 ± 20.52	0.59
pNN50 (%)	53.35 ± 20.57	55.10 ± 33.08	0.83	45.90 ± 24.70	47.30 ± 31.19	0.87

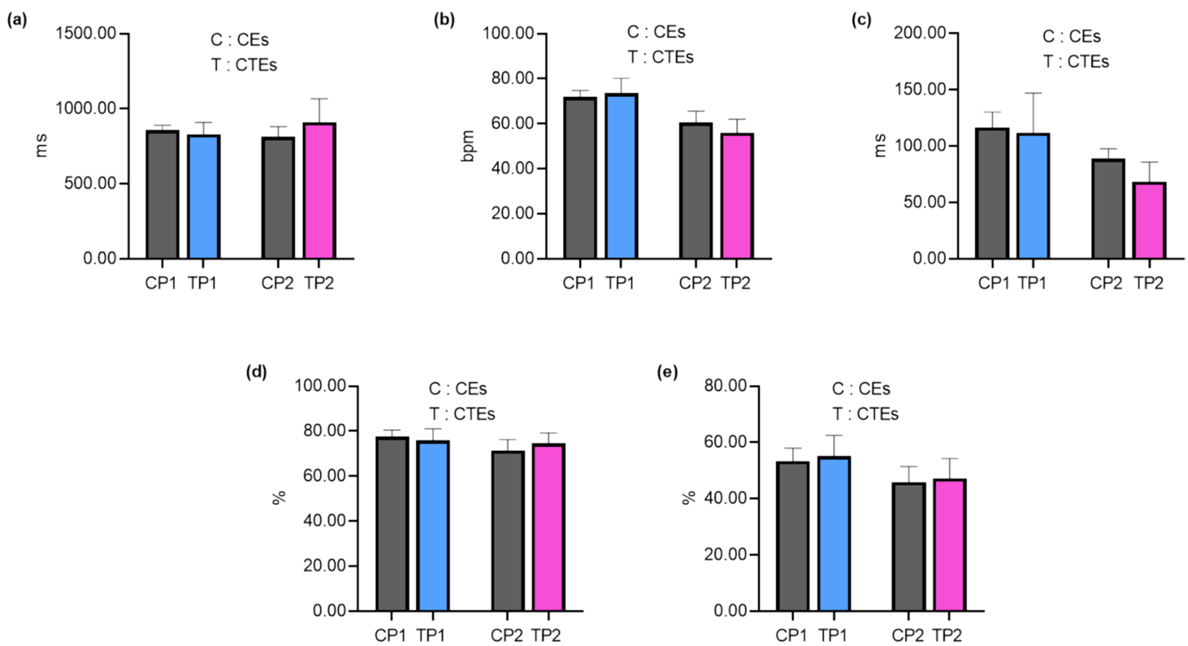

Fig. 5 Comparative analysis of mean data using CEs and CTEs in position 1 (P1) and position 2 (P2) in the time-domain of HRV **a** AvgRR **b** AvgHR **c** SDNN **d** pNN20 **e** pNN50

results of the paired *t*-tests. A comparative analysis of the means are presented in Fig. 5.

3.2.1 CEs vs CTEs in position 1

The AvgRR was calculated for both electrodes in position 1. The results indicated no significant differences between CEs (857.88 ± 144.74 ms) and CTEs (830.25 ± 353.32 ms) with $p = 0.72$. Similarly, there was no significant difference in the AvgHR values between CEs (71.94 ± 12.92 bpm) and CTEs (73.51 ± 30.12 bpm) with $p = 0.82$. There was no significant difference for the SDNN between CEs (116.58 ± 61.11 ms) and CTEs (111.85 ± 156.90 ms) with $p = 0.89$. Likewise, pNN20 and pNN50 had no significant differences between CEs (75.95 ± 23.23%; 53.35 ± 20.57%) and CTEs (77.50 ± 13.38%; 55.10 ± 33.08%) with $p = 0.73$ and $p = 0.83$, respectively.

3.2.2 CEs vs CTEs in position 2

For position 2, AvgRR had no significant difference between CEs (814.73 ± 302.05 ms) and CTEs (911.52 ± 695.72 ms) with $p = 0.51$. AvgHR showed no significant difference between CEs (60.66 ± 22.35 bpm) and CTEs (56.02 ± 27.02 bpm) with $p = 0.49$. SDNN exhibited no significant difference between CEs (88.99 ± 38.84 ms) and CTEs (68.46 ± 77.61 ms) with $p = 0.26$. For pNN20 and pNN50, no significant differences were found between CEs (71.35 ± 21.75%; 45.90 ± 24.70%) and CTEs (74.65 ± 20.52%; 47.30 ± 31.19%) with $p = 0.59$ and $p = 0.87$, respectively.

3.3 Nonlinearity

We also show the efficiency of CTEs, in acquiring data by comparing it with CEs from a nonlinear perspective, using

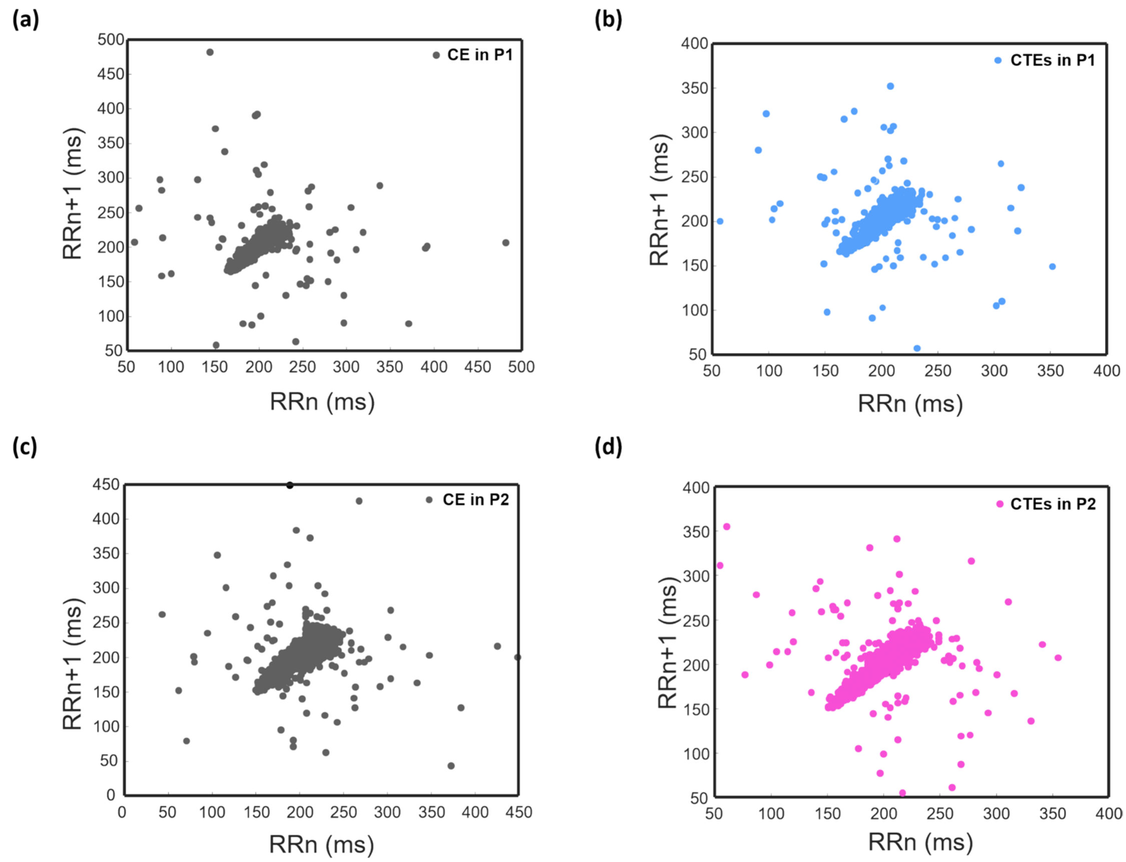

Fig. 6 Poincaré plots using **a** CE and **b** CTEs in position 1 (P1) **c** CE and **d** CTEs in position 2 (P2)

Table 2 Quantitative results of the Poincaré analysis

	Position 1		Position 2	
	CE	CTEs	CE	CTEs
SD1 (ms)	78.04	61.48	87.07	76.20
SD2 (ms)	49.38	33.78	76.74	84.46
SD1/SD2	1.58	1.82	1.13	0.90

a Poincaré plot (Fig. 6) for one subject. We conducted a quantitative analysis of the R-R interval time series using the Poincaré plot, and the results of the determined parameters are presented in Table 2.

Visually, the Poincaré plots were narrower when CE was used in positions 1 and 2 compared to CTEs. However, similar patterns of scatter are observed with both electrodes in the two positions. Minimal differences are also observed in the dispersion and clustering of points.

3.4 Position effect of the CTEs group

An evaluation of the position effect within the CTEs group was considered. Comparison between positions 1 and 2 revealed no significant differences (Table 3) in the time-domain HRV indices ($p > 0.05$ for all parameters).

Table 3 Results of the position effect between the CTE groups

Parameter	AvgRR (ms)	AvgHR (bpm)	SDNN (ms)	pNN20 (%)	pNN50 (%)
p value	0.97	0.07	0.57	0.54	0.22

4 Discussion

Herein, CTEs were quantitatively compared to CEs via their ECG morphologies and time-series HRV analysis. The positions for the CTEs were varied in two experiments. Our findings affirm the potential of CTEs for ECG acquisition and also identifies the most suitable electrode position for the application of CTEs.

A fundamental feature of a quality ECG signal is one that is free from any erroneously detected R peaks caused by significant distortion or contains no absent R peaks. From Figs. 3 and 4, CTEs exhibited superior R peak characteristics in ECG waveforms compared to CEs. The enhanced R peak amplitude and clarity observed in CTE-based ECG recordings suggest improved signal quality and accuracy. This is particularly useful as R peak identification is key for reliable cardiac monitoring and arrhythmia diagnosis [30–32]. Previous research has highlighted the limitations of CEs, including motion artefacts [17, 33] and signal degradation [34–36], which can compromise R peak detection and analysis. In contrast, the CTEs exhibit improved conductivity and reduced noise sensitivity, resulting in an enhanced ECG signal quality.

The R peak, indicative of ventricular depolarisation and the onset of ventricular contraction, was clearly discernible in ECG signals recorded using CTEs, as illustrated in Figs. 3 and 4. The waveforms obtained from CTEs showed well-defined P, QRS, and T points, which were more prominent compared to those captured by CEs. This clarity is fundamental for accurate HRV analysis, as it helps in distinguishing the R peak from other waveforms and minimises processing errors. Following filtering, substantial improvements in SNR were observed: for the CE in position 1, SNR improved from 8.71 dB to 17.50 dB; for the CTEs in position 1, SNR increased from 6.95 dB to 15.39 dB; for the CE in position 2, SNR increased from 9.31 dB to 17.97 dB and for the CTEs in position 2, SNR rose from 8.71 dB to 16.78 dB. These results affirm the effectiveness of the filtering techniques and validate the data provided by the CTEs, proving the efficacy of our material.

The heart's ability to adapt to changing circumstances by quickly identifying and responding to unpredictable stimuli is measured by HRV [37]. Time-domain indices of HRV serve as an indicator of autonomic homeostasis, particularly in evaluating the mental and metabolic well-being of an individual. In this study, time-domain indices of HRV were used to compare CTEs and CEs (Table 1). Despite the distinct material compositions and observable variations in mean values, the paired *t*-test failed to detect significant differences ($p > 0.05$) in AvgRR, AvgHR, SDNN, pNN20 and pNN50 between the two electrodes in positions 1 and 2. This outcome may seem counterintuitive, given our expectation that CTEs would outperform CEs. However, these results actually reveal that CTEs are as equally competent as CEs in terms of these specific HRV parameters. This indicates that CTEs serve as a viable alternative to CEs for HRV assessments, offering advantages such as cost-effectiveness and enhanced comfort without compromising measurement accuracy. Generally, Ag/AgCl electrodes have been regarded as the gold standard in ECG recordings due to their reliability and accuracy. In contrast, the utilisation of CTEs offer not only the supplementary benefit of enhanced comfort but also demonstrates notable advancements in accuracy and reliability, as corroborated by the ECG morphologies.

The derivation of HRV stems from the intricate interplay of diverse physiological mechanisms, signifying the involvement of nonlinear systems in the regulation of heart rate [37–39]. Thus, it stands to reason that, assessing the efficacy of CTEs involves a comprehensive examination of its impact on nonlinearity. Consequently, an analysis employing Poincaré plots was conducted to explore the nonlinear dynamics governing heart rate regulation and to elucidate any discernible variations facilitated by the use of the CTEs. In comparing the performance of CEs to CTEs across positions 1 and 2 from the Poincaré plots (Fig. 6), it is apparent that both electrodes exhibit scatters characterised by analogous patterns. Also, minimal disparities are noted in terms of the dispersion and clustering of data points. These observations suggest that, in terms of nonlinearity, CTEs perform comparably to CEs, indicating the robustness and consistency of its performance across different electrode positions. This further highlights the potential efficacy of CTEs in impacting physiological responses, and overall wellbeing. Moreover, it suggests that the electrical conductivity and signal quality of CTEs are sufficient to capture subtle beat-to-beat variability in heart rate, akin to CEs. Through these, we can intuitively confirm that our CTE is capable of ECG measurement and that the obtained data are reliable.

Another important implication of our findings is the stability of the CTEs across different electrode positions. The lack of significant differences between the two positions (Table 3) reveal that CTE maintains its performance irrespective of placement variability. Nonetheless, based on literature and practical considerations, we opt for position 2. Previous studies using CTEs in the pillow (nape/head) and foot mat (leg) [40, 41] have yielded favourable outcomes. During long-term ECG monitoring, specifically during sleep, individuals change positions, causing frequent movement of the hands, which can lead to electrode displacement and signal distortion. The nape provides a relatively stationary surface due to the position of the head throughout most sleep stages, ensuring consistent electrode contact. Similarly, while leg movements may occur, they are often less disruptive to electrode placement compared to hand movements, and may be helpful predictors of cardiovascular diseases caused by periodic limb movement during sleep [42–44], especially in the elderly. From a practical standpoint, selecting the nape and legs for electrode placement eases the integration of monitoring systems into bedding. Integrating electrodes into pillows and bedding allows for unobtrusive and continuous monitoring, without the need for additional wearable devices. This promotes user comfort and compliance. Furthermore, this configuration enables seamless data collection in research and clinical settings, enhancing the feasibility and reliability of sleep studies and diagnostic assessments.

5 Conclusion

ECG signals are instrumental in assessing physiological states and predicting health risks. CTEs improve upon traditional electrodes by reducing inconvenience and signal variability, allowing for easier ECG monitoring from various body parts without complex attachment procedures. Their deformable nature supports better integration into daily life and encourages consistent monitoring. Beyond these advantages, CTEs have potential for broader applications, such as developing a “lonely death prevention system” that monitors health and issues emergency alerts. Future research should focus on incorporating advanced algorithms for real-time analysis and predictive modelling. Additionally, integrating CTEs with other wearable technologies and telehealth platforms could further enhance remote monitoring and patient outcomes.

Acknowledgements The authors would like to thank the Korea Foundation for International Healthcare (KOFIH) and the Dr. LEE Jong-wook Fellowship team for the support. This research was supported by the Regional Innovation Strategy (RIS) through the National Research Foundation of Korea (NRF), funded by the Ministry of Education (MOE) in 2024 (2022RIS-005) and the National Research Foundation of Korea (NRF) grant funded by the Korea government (MSIT) (No.RS-2023-00221762). We also appreciate MEZOO Co. Ltd for the device and Ezekiel E. Nettey-Oppong for his assistance.

Author contributions L.A. Asante, S.B. Park and H.S. Kim contributed to the study conception and design. The data collection was done by L.A. Asante. The data analysis was performed by L.A. Asante, S. Cho and J. Choi. L.A. Asante wrote the first draft of the manuscript, and all authors edited and reviewed the manuscript. H.S. Kim supervised and directed the entire study process. All authors read and approved the final manuscript.

Funding This research was supported by the “Regional Innovation Strategy (RIS)” through the National Research Foundation of Korea (NRF) funded by the Ministry of Education (MOE) in 2024 (2022RIS-005) and the National Research Foundation of Korea (NRF) grant funded by the Korea government (MSIT) (No.RS-2023–00221762).

Declarations

Conflict of interest The authors have no pertinent financial or non-financial interests to disclose.

Ethical approval The experimental procedures were approved by the Institutional Review Board of Yonsei University Mirae Campus (1041849–202403-BM-057–01).

Consent to participate Informed consent was obtained from all participants included in the study.

Consent for publication Not applicable.

References

1. Kwon MH, Kwon YE. A Study on the subjectivity of the elderly who live alone caregivers in perception of lonely death. Korean J Adult Nurs. 2012;24(6):647–58. https://doi.org/10.7475/kjan.2012.24.6.647.
2. Králová J. What is social death? Contemp Soc Sci. 2015;10(3):235–48. https://doi.org/10.1080/21582041.2015.1114407.
3. Caswell G, O’Connor M. Agency in the context of social death: dying alone at home. In: Králová J, Walter T(eds.) Social death: Questioning the life-death boundary; Routledge: 2018. pp. 27–399
4. Borgstrom, E. Social death in end-of-life care policy. In: Social death: Questioning the life-death boundary; Routledge: 2018. pp. 50–61.
5. Lee J, Cohen PN, Lee Mj, Woo H. Lone death in South Korea: Exploring community level factors on lone death in South Korea.
6. Kim HS. Analysis of dying alone among media reports. Asia pac J Psychol Couns. 2017;1:3540. https://doi.org/10.21742/apjpc.2017.1.1.06.
7. Yeung, J.S., Yoonjung. South Korea’s middle aged men are dying ‘lonely deaths’. Available online: https://edition.cnn.com/2022/12/18/asia/south-korea-godoksa-lonely-death-intl-hnk-dst/index.html Accessed on 2 Apr.
8. Dey R, Samanta PK, Chokda RP, De BP, Appasani B, Srinivasulu A, Philibert N. Graphene-based electrodes for ECG signal monitoring: fabrication methodologies, challenges and future directions. Cogent Eng. 2023;10:2246750. https://doi.org/10.1080/23311916.2023.2246750.
9. Wartzek T, Lammersen T, Eilebrecht B, Walter M, Leonhardt S. Triboelectricity in capacitive biopotential measurements. IEEE Trans Biomed Eng. 2010;58:1268–77. https://doi.org/10.1109/TBME.2010.2100393.
10. Lulai LM, Guo S, Worswick S, DeLeo VA, Adler BL. Contact dermatitis in the inpatient hospital setting–an updated review of the literature. Curr Dermatol Rep. 2022;11:179–93. https://doi.org/10.1007/s13671-022-00366-5.
11. Myers J, Arena R, Franklin B, Pina I, Kraus WE, McInnis K, Balady GJ. Recommendations for clinical exercise laboratories: a scientific statement from the American Heart Association. Circulation. 2009;119:3144–61. https://doi.org/10.1161/CIRCULATIONAHA.109.192520.
12. Sandau KE, Funk M, Auerbach A, Barsness GW, Blum K, Cvach M, Lampert R, May JL, McDaniel GM, Perez MV. Update to practice standards for electrocardiographic monitoring in hospital settings: a scientific statement from the American Heart Association. Circulation. 2017;136:e273–344. https://doi.org/10.1161/CIR.0000000000000527.
13. Heo JS, Eom J, Kim YH, Park SK. Recent progress of textile-based wearable electronics: a comprehensive review of materials, devices, and applications. Small. 2018;14:1703034. https://doi.org/10.1002/smll.201703034.
14. Ismar E, KurşunBahadir S, Kalaoglu F, Koncar V. Futuristic clothes: Electronic textiles and wearable technologies. Global Chall. 2020;4:1900092. https://doi.org/10.1002/gch2.201900092.
15. Lee I, Shin S, Jang Y, Song Y, Jeong JW, Kim S. Comparison of conductive fabric sensor and Ag-AgCl sensor under motion artifacts. In: Proceedings of the 2008 30th annual international conference of the IEEE engineering in medicine and biology society, 2008. pp. 1300–3.
16. Lee E, Kim I, Liu H, Cho G. Exploration of AgNW/PU nanoweb as ECG textile electrodes and comparison with Ag/AgCl electrodes. Fibers Polym. 2017;18:1749–53. https://doi.org/10.1007/s12221-017-7410-6.
17. Qin Q, Li J, Yao S, Liu C, Huang H, Zhu Y. Electrocardiogram of a silver nanowire based dry electrode: quantitative comparison with the standard Ag/AgCl gel electrode. IEEE Access. 2019;7:20789–800. https://doi.org/10.1109/access.2019.2897590.
18. Malik M. Heart rate variability: Standards of measurement, physiological interpretation, and clinical use: Task force of the

European Society of Cardiology and the North American Society for Pacing and Electrophysiology. Ann Noninvasive Electrocardiol. 1996;1:151–81. https://doi.org/10.1111/j.1542-474x.1996.tb00275.x.

19 Pan J, Tompkins WJ. A real-time QRS detection algorithm. IEEE trans biomed Eng. 1985. https://doi.org/10.1109/tbme.1985.325532.

20. Schafer RW. What is a Savitzky-Golay filter?[lecture notes]. IEEE Signal Process Mag. 2011;28:111–7. https://doi.org/10.1109/msp.2011.941097.

21 Shaffer F, Ginsberg JP. An overview of heart rate variability metrics and norms. Front Pub Heal. 2017. https://doi.org/10.3389/fpubh.2017.00258.

22. Hamilton PS, Tompkins WJ. Quantitative investigation of QRS detection rules using the MIT/BIH arrhythmia database. IEEE Trans Biomed Eng. 1986;BME-33(12):1157–65. https://doi.org/10.1109/TBME.1986.325695.

23. Woo MA, Stevenson WG, Moser DK, Middlekauff HR. Complex heart rate variability and serum norepinephrine levels in patients with advanced heart failure. J Am Coll Cardiol. 1994;23:565–9. https://doi.org/10.1016/0735-1097(94)90737-4.

24 Rajendra Acharya U, Suri JS, Spaan JAE, Krishnan SM, editors. Advances in cardiac signal processing. Berlin, Heidelberg: Springer Berlin Heidelberg; 2007. https://doi.org/10.1007/978-3-540-36675-1.

25. Ciccone AB, Siedlik JA, Wecht JM, Deckert JA, Nguyen ND, Weir JP. Reminder: RMSSD and SD1 are identical heart rate variability metrics. Muscle Nerve. 2017;56:674–8. https://doi.org/10.1002/mus.25573.

26. Tulppo MP, Makikallio TH, Seppänen T, Laukkanen RT, Huikuri HV. Vagal modulation of heart rate during exercise: effects of age and physical fitness. Am J Physiol Heart Circ Physiol. 1998;274:H424–9. https://doi.org/10.1152/ajpheart.1998.274.2.H424.

27. Brennan M, Palaniswami M, Kamen P. Poincaré plot interpretation using a physiological model of HRV based on a network of oscillators. Am J Physiol Heart Circ Physiol. 2002;283:H1873–86. https://doi.org/10.1152/ajpheart.00405.2000.

28. Bansal D, Khan M, Salhan A. A review of measurement and analysis of heart rate variability. In: Proceedings of the 2009 international conference on computer and automation engineering, 2009. pp. 243–6.

29. Chatterjee S, Thakur RS, Yadav RN, Gupta L, Raghuvanshi DK. Review of noise removal techniques in ECG signals. IET Signal Proc. 2020;14:569–90. https://doi.org/10.1049/iet-spr.2020.0104.

30. Liu X, Yang J, Zhu X, Zhou S, Wang H, Zhang H. A novel R-peak detection method combining energy and wavelet transform in electrocardiogram signal. Biomed Eng Appl Basis Commun. 2014;26:1450007. https://doi.org/10.4015/s1016237214500070.

31. Kaya Y, Pehlivan H, Tenekeci M. Effective ECG beat classification using higher order statistic features and genetic feature selection. Biomed Res India. 2017;28(17):7594–603.

32. Sharma T, Sharma KK. QRS complex detection in ECG signals using locally adaptive weighted total variation denoising. Comput Biol Med. 2017;87:187–99. https://doi.org/10.1016/j.compbiomed.2017.05.027.

33. Lo L-W, Zhao J, Aono K, Li W, Wen Z, Pizzella S, Wang Y, Chakrabartty S, Wang C. Stretchable sponge electrodes for long-term and motion-artifact-tolerant recording of high-quality electrophysiologic signals. ACS Nano. 2022;16:11792–801. https://doi.org/10.1021/acsnano.2c04962.

34. Sekitani T, Yokota T, Kuribara K, Kaltenbrunner M, Fukushima T, Inoue Y, Sekino M, Isoyama T, Abe Y, Onodera H. Ultraflexible organic amplifier with biocompatible gel electrodes. Nat Commun. 2016;7:11425. https://doi.org/10.1038/ncomms11425.

35. Zhang N, Yue L, Xie Y, Samuel OW, Omisore OM, Pei W, Xing X, Lin C, Zheng Y, Wang L. A novel antibacterial membrane electrode based on bacterial cellulose/polyaniline/$AgNO_3$ composite for bio-potential signal monitoring. IEEE J transl Eng Health Med. 2018;6:1–10. https://doi.org/10.1109/jtehm.2018.2863388.

36. Satti AT, Park J, Park J, Kim H, Cho S. Fabrication of parylene-coated microneedle array electrode for wearable ECG device. Sensors. 2020;20:5183. https://doi.org/10.3390/s20185183.

37. Rajendra Acharya U, Paul Joseph K, Kannathal N, Lim CM, Suri JS. Heart rate variability: a review. Med Biol Eng Compu. 2006;44:1031–51. https://doi.org/10.1007/s11517-006-0119-0.

38. Ziegler D, Piolot R, Strassburger K, Lambeck H, Dannehl K. Normal ranges and reproducibility of statistical, geometric, frequency domain, and non-linear measures of 24-hour heart rate variability. Horm Metab Res. 1999;31:672–9. https://doi.org/10.1055/s-2007-978819.

39. Roy B, Ghatak S. Nonlinear methods to assess changes in heart rate variability in type 2 diabetic patients. Arq Bras Cardiol. 2013;101:317–27. https://doi.org/10.5935/abc.20130181.

40. Ishijima M. Cardiopulmonary monitoring by textile electrodes without subject-awareness of being monitored. Med Biol Eng Compu. 1997;35:685–90. https://doi.org/10.1007/bf02510978.

41. Devot S, Bianchi AM, Naujoka E, Mendez MO, Brauers A, Cerutti S. Sleep monitoring through a textile recording system. In: Proceedings of the 2007 29th annual international conference of the IEEE engineering in medicine and biology society, 2007. pp. 2560–3.

42. Mirza M, Shen W-K, Sofi A, Jahangir A, Mori N, Tajik AJ, Jahangir A. Frequent periodic leg movement during sleep is associated with left ventricular hypertrophy and adverse cardiovascular outcomes. J Am Soc Echocardiogr. 2013;26:783–90. https://doi.org/10.1016/j.echo.2013.03.018.

43. Figorilli M, Puligheddu M, Congiu P, Ferri R. The clinical importance of periodic leg movements in sleep. Curr Treat Options Neurol. 2017;19:1–15. https://doi.org/10.1007/s11940-017-0446-5.

44. Huang TC, Tseng PT, Wu MN, Stubbs B, Carvalho AF, Lin PY, Chen YW, Chen TY, Hsu CY. Periodic limb movements during sleep are associated with cardiovascular diseases: a systematic review and meta-analysis. J Sleep Res. 2019;28:e12720. https://doi.org/10.1111/jsr.12720.